SANDIA REPORT
SAND2001-1629
Unlimited Release
Printed June 2001

Evolution of Stress in ScD_2/Cr Thin Films Fabricated by Evaporation and High Temperature Reaction

David P. Adams, Laurence E. Brown, Ronald Goeke, Juan A. Romero, Beverly Silva

Prepared by
Sandia National Laboratories
Albuquerque, New Mexico 87185 and Livermore, California 94550

Sandia is a multiprogram laboratory operated by Sandia Corporation, a Lockheed Martin Company, for the United States Department of Energy under Contract DE-AC04-94AL85000.

Issued by Sandia National Laboratories, operated for the United States Department of Energy by Sandia Corporation.

Available to DOE and DOE contractors from
U.S. Department of Energy
Office of Scientific and Technical Information
P.O. Box 62
Oak Ridge, TN 37831

Telephone: (865)576-8401
Facsimile: (865)576-5728
E-Mail: reports@adonis.osti.gov
Online ordering: http://www.doe.gov/bridge

Available to the public from
U.S. Department of Commerce
National Technical Information Service
5285 Port Royal Rd
Springfield, VA 22161

Telephone: (800)553-6847
Facsimile: (703)605-6900
E-Mail: orders@ntis.fedworld.gov
Online order: http://www.ntis.gov/ordering.htm

SAND2001-1629

Unlimited Release
Printed June 2001

Evolution of Stress in ScD_2 /Cr Thin Films Fabricated by Evaporation and High Temperature Reaction

David P. Adams, Laurence E. Brown, Ronald Goeke
Juan A. Romero, Beverly Silva

Thin Film, Vacuum and Packaging Department
Sandia National Laboratories
P.O. Box 5800
Albuquerque, NM, 87185-0959

Abstract

The stress of scandium dideuteride, ScD_2, thin films is investigated during each stage of vacuum processing including metal deposition via evaporation, reaction and cooldown. ScD_2 films with thin Cr underlayers are fabricated on three different substrate materials: molybdenum-alumina cermet, single crystal sapphire and quartz. In all experiments, the evaporated Cr and Sc metal is relatively stress-free. However, reaction of scandium metal with deuterium at elevated temperature to form a stoichiometric dideuteride phase leads to a large compressive in-plane film stress. Compression during hydriding results from an increased atomic density compared with the as-deposited metal film. After reaction with deuterium, samples are cooled to ambient temperature, and a tensile stress develops due to mismatched coefficients of thermal expansion (CTE) of the substrate-film couple. The residual film stress and the propensity for films to crack during cooldown depends principally on the substrate material when using identical process parameters. Films deposited onto quartz substrates show evidence of stress relief during cooldown due to a large CTE misfit; this is correlated with crack nucleation and propagation within films. All ScD_2 layers remain in a state of tension when cooled to 30^{o}C. An *in-situ*, laser-based, wafer curvature sensor is designed and implemented for studies of ScD_2 film stress during processing. This instrument uses a two-dimensional array of laser beams to noninvasively monitor stress during sample rotation and with samples stationary. Film stress is monitored by scattering light off the backside of substrates, i.e., side opposite of the deposition flux.

Purpose of Report

The purpose of this report is to document the characterization and the analysis of stress generated in ScD_2/Cr thin films grown onto various substrates. This multilayer film is important for NT/NGs, and it is expected that the reliability of this coating is influenced by the stress state changes that occur over time. This report is intended to serve as a comprehensive source of information regarding thin film stress generated during processing and its dependence on substrate material. The analytical instrument used for measurements of stress is recommended for production.

Section I. Introduction: Thin film stress and techniques for measuring this property

Stress is considered critical to the reliability and performance of numerous thin films, including rare earth metal hydrides. Although a few applications benefit from a controlled, low amount of strain, excessive film stress most often compromises adhesion to a substrate. Films may plastically yield due to significant amounts of stress, but, in many cases, coatings detach from a wafer due to insufficient interfacial toughness. This is unacceptable for applications that require a thin film to remain intact during operation. Stress is a material property that can, if uncontrolled, lead to the rejection of an entire production lot.

In general, two nonzero stress 'types' characterize thin films. This includes compressive and tensile stress. Both types of stress can develop during film fabrication or operation, and each may degrade the mechanical stability of a coating. It is well-known that stress causes a number of microstructural or morphological changes. If sufficiently large, compressive stress leads to film decohesion. This is characterized by blisters or buckles (sometimes cracked) that extend across a wafer. Large tensile stress generates cracks, and fracture may occur within a film or a substrate. If uncontrolled, both types of stress lead to complete spallation.

As a first step in optimizing the reliability of a thin film, it is essential to understand the development of film stress during fabrication. Subtle changes in process parameters, such as temperature, can influence the microstructure or morphology, and these in turn affect film stress. Film structure (and stress) can also be affected by the

substrate to which it is constrained. In general, thin films may attempt to replicate the substrate surface structure or intermix with the underlying material leading to differences in stress magnitude. The stress developed during processing is often distinguished in terms of intrinsic and extrinsic effects. Intrinsic stress is related to the density and microstructure of a layer. It can develop due to changes in the number of point, line and planar defects per unit volume, grain structure, phase and lattice type. Because microstructure depends sensitively on the process conditions (source/substrate geometry, growth temperature and deposition rate), intrinsic stress is directly affected by the growth parameters. Extrinsic stress, on the other hand, develops from the thermomechanical behavior of a thin film-substrate couple. Often thin films are deposited at high temperature and then cooled prior to removal from a vacuum system. If a film and substrate are dissimilar materials, a change in temperature can generate significant extrinsic stress due to a mismatch in coefficients of thermal expansion. Films change lattice parameter at a different rate than substrates, leading to a residual stress. Note, generation of extrinsic stress can also occur during high temperature operation of a thin film. Applications that require high temperature excursions or isothermal anneals are subject to changes in stress, and, once cooled, films may return to a stress state different than that prior to heating.

In current work, we investigate the stress developed solely during processing of ScD_2/Cr thin films. The development of stress during each stage of metal hydride processing is of interest, since large changes may occur during growth, reaction or cooldown that compromise adhesion. Previous analysis involving nanoindentation and x-ray diffraction shows that ScD_2 thin films processed onto cermet substrates (with surfaces prepared by high temperature bakes) are in a state of tension after growth.[1]

An *in-situ* probe of thin film stress is therefore desired to sensitively monitor the properties of a film contained within the vacuum processing apparatus. This instrument must noninvasively 'peer' into the chamber and relay details about a film to the operator. Analysis must not affect the growth process by heating substrates or inducing undesired chemical reactions. The analytical technique must, however, be sensitive, since changes in stress can rapidly occur over fractions of a second. *In-situ* monitoring procedures for

real-time process control potentially provide a means to evaluate deposition parameters and prevent product loss.

A number of analytical techniques are capable of probing thin film stress *in-situ*. For example, diffraction-based techniques including conventional x-ray diffraction, grazing incidence x-ray scattering (GIXS), and reflection high-energy electron diffraction (RHEED) are commonly used in research laboratories. These techniques are used to determine strain – the deviation of a film's lattice parameters from known equilibrium values. For the purpose of probing ScD_2 thin film processes involving sample rotation, diffraction-based techniques are considered difficult. Although these techniques are extremely powerful, the precise geometry required for analysis is difficult to maintain, particularly with moving samples. We envision that a 'stop and go' procedure would be required for analysis when using these techniques. However, interruption of a growth process is undesired, for isothermal anneals can change microstructure.

Instead, a wafer curvature measurement technique is used. Wafer curvature techniques[2] are attractive for determining thin film stress in a manufacturing setting with moving samples. In general, a number of methods have been devised including x-ray techniques (double crystal diffraction topography) [3] and a variety of laser based diagnostics that operate at optical wavelengths. Each of these probe substrate shape before, during and after thin film growth, and stress can be calculated from measured curvature changes if certain conditions are maintained. Laser-based instruments are beneficial, because they are noninvasive, sensitive and simpler to operate than x-ray techniques. Typically light enters through a viewport, strikes a sample and returns to a camera for analysis. The radiant power impinging on a sample is a few microWatts, insufficient to cause significant heating. In most cases, the entire laser apparatus is maintained external to the vacuum. Only a clear viewport and a direct line to a sample is required. Several forms of laser-based, light scattering instruments have been investigated previously. These include laser scanners, which steer a beam of light across a wafer to determine curvature. This has high sensitivity for benchtop experiments, but is considered slow for growth processes involving moving substrates.

For the present work, a multi-beam, optical stress sensor (referred to as MOSS^{TM}) is used. This technique is originally developed by E. Chason, J.A. Floro et. al. at Sandia

National Laboratories[4] and commercialized by k-Space Associates, Inc. (Ann Arbor, MI). The technique involves directing an array of laser light spots onto a substrate in order to accurately map curvature, and stress is determined via Stoney's[5] or other formulation. The MOSS technique is an improvement over other optical analysis techniques, because it simultaneously illuminates a substrate with an array of beams. Multiple beams of light are reflected from a sample without the need for mechanical raster, thus allowing rapid detection. The technique also allows for a sensitive measurement of stress, because noise introduced from vibrating pumps, heaters, etc. is overcome. Because an array of laser spots is deflected uniformly during vibration, the effects of noise on curvature measurements are significantly reduced. Sensitive measurements of stress have been conducted on a number of thin film systems using the MOSS technique. These include measurements of stress in layers as thin as 0.1 monolayers (Ge on a Si(001)).[6] Recent work by Hearne et. al.[7] probes stress during deposition and temperature cycling, while a previous laboratory directed research and development (LDRD) study demonstrates the feasibility of monitoring metal hydride films with this technique.[8]

Section II. Thin film processing system and analysis equipment

Vacuum apparatus for fabrication of ScD_2 thin films

ScD_2 films are fabricated using a two-step process involving evaporation of Sc followed by reaction at elevated temperature with high purity D_2 gas. Both procedures are conducted in the same vacuum apparatus, and high purity Sc and D_2 are used because of the strong affinity of this metal to oxygen. Measures such as bakeout are taken to ensure that the system is clean prior to growth.

The system used for fabricating ScD_2 thin films is a UHV cryopumped apparatus referred to as 'Evap 1' (see Figure 1). The chamber is a water-cooled, stainless steel, vertical cylinder with a volume of 60 liters. While the system is designed for all metal seals, a Viton o-ring is used on the lid seal throughout these experiments. All other seals remain metal. The system is roughed entirely with dry vacuum pumps to < 50 mTorr

before crossing over to a CTI Cryogenics CT8 cryopump. Typical base pressure attained after an overnight bakeout is $<10^{-8}$ Torr.

Material deposition is achieved by evaporation from two single-pocket electron beam evaporators located side by side in the bottom of the vacuum chamber. For all experiments a Cr layer is first deposited followed by a thicker Sc coating. The two guns share the same 10kV power supply, so only one can be operated at a time. A crystal monitor rate controller regulates e-gun power for a constant deposition rate. The controller also times the shutter to open after the deposition material reaches evaporation temperature and to close when the desired thickness is reached.

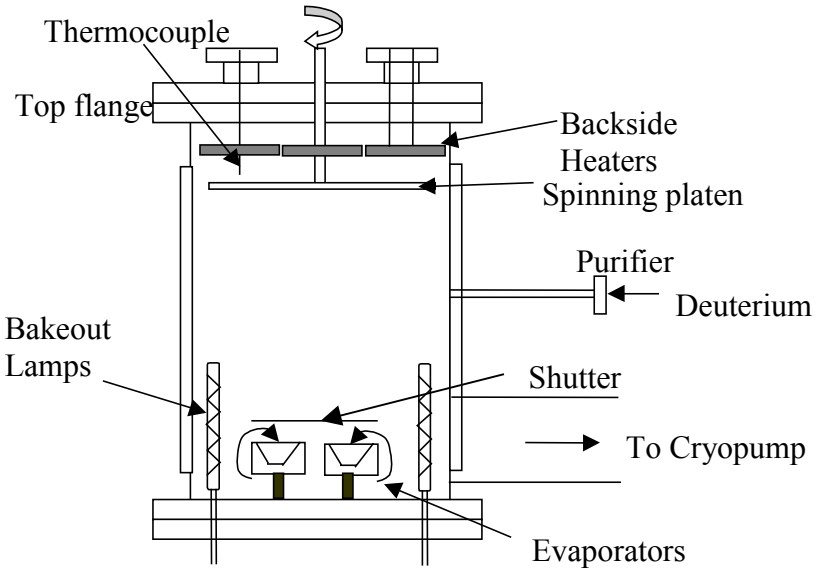

Figure 1 Schematic of UHV chamber apparatus.

Substrates rest on a stainless steel platen that is rotated by a UHV bellows type feedthrough located in the center of the top plate. Parts are rotated to improve the deposition uniformity and provide uniform heating. This platen can hold up to 20 1.5”diameter substrates and is made planar with the top plate flange for ease of laser alignment. The chamber has two forms of heating. Substrate heating is provided by three 10cm Boron Nitride-encased graphite heaters located behind the wafers at a spacing of 3cm. These heaters are controlled by closed loop temperature feedback from a type K thermocouple located 6mm from the backside of the platen. Two infrared bakeout lamps

located in the bottom of the chamber accomplish chamber bakeout. Prior to each process run the chamber is baked out overnight at a substrate temperature of 200ºC and a wall temperature near 100ºC.

Deuterium is introduced into the same chamber apparatus in order to convert as-deposited scandium metal films to stoichiometric ScD_2. Gas is delivered to the middle of the chamber through a 3/8" stainless steel tube after passing through a palladium membrane purifier. The purity of the initial gas is 99.9995% research grade deuterium. Vendor specifications indicate impurity levels of < 1 ppm H_2O, < 1 ppm O_2, and < 1 ppb hydrocarbons/halocarbons as delivered from the purifier. The flow rate is calibrated for a clean empty chamber in which the pressure rises linearly with time. The purifier is operated at 400ºC, and a constant pressure of 12 psig on the upstream side delivers a repeatable flow rate of 8.8 Torr-L/s. However, with metal coatings having a strong affinity for D present on the walls and fixtures after deposition, no pressure rise is observed initially. A slow transition to a linear pressure rise is observed after 2.5 minutes as indicated in Figure 2. A final pressure of ~ 12 Torr is reached at the end of gas introduction.

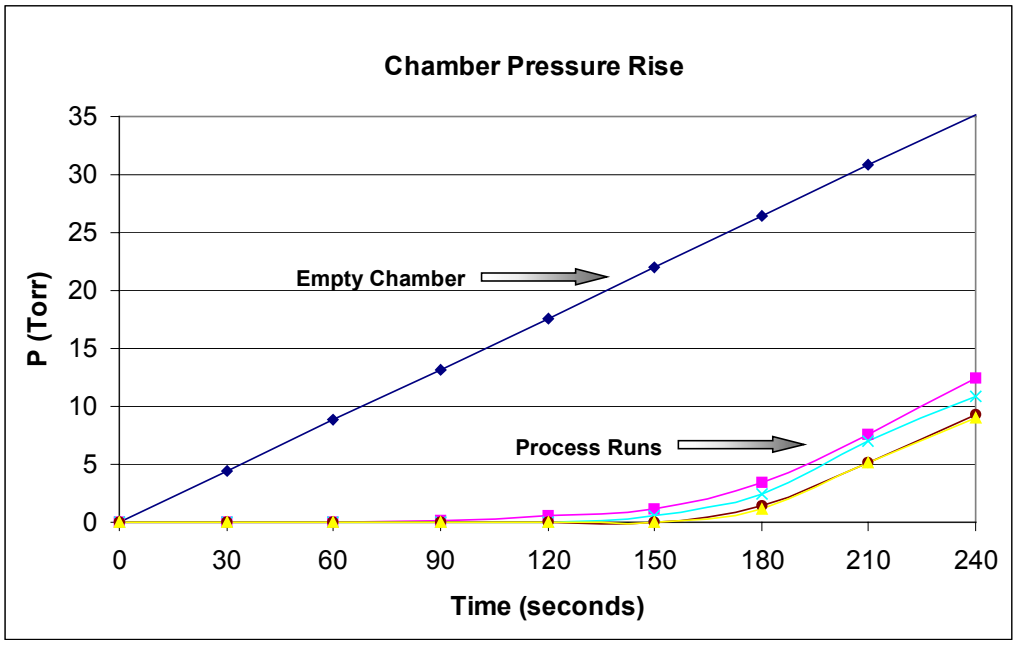

Figure 2 Plot of deuterium pressure in chamber after opening valve. 'Empty chamber' curve refers to not having deposited Sc prior to gas entry.

Since the deuterium-loaded metal will outgas upon subsequent heating (e.g., during bakeout), all shields and fixtures are replaced after each run. These parts are stripped of chromium and scandium with a dilute ceric ammonium nitrate solution and rinsed. All parts are then solvent cleaned, followed by a bake in hydrogen and in vacuum to 800ºC prior to returning for use in the evaporator system.

Design of multi-beam stress sensor and long working distance, optical microscope

A multi-beam wafer curvature apparatus is designed for incorporation onto the Evap 1 system to probe ScD_2/Cr film stress. This sensor is manufactured by k-Space Associates and consists of a semiconductor diode laser, several optical elements, a high-speed charge coupled device (CCD) camera, a rotary encoder, and computer with control boards. As shown in Figure 3, the instrument operates by directing an array of laser light spots through a 8.57 cm (3.375") O.D. viewport mounted on the vacuum system. This

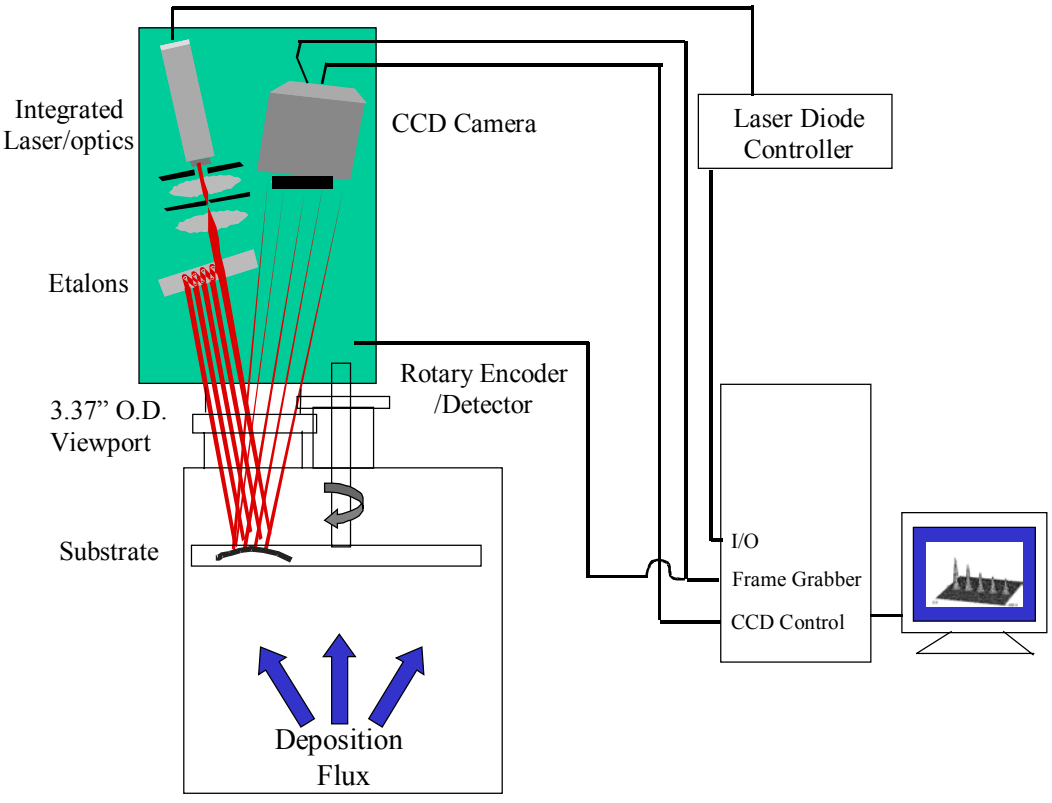

Figure 3 Multibeam optical stress sensor schematic.

viewport is kept at ~ 30^{o}C during deposition and reaction. For analysis, it is critical not to clamp a wafer, since it must respond to the stress accumulated in the thin film.

We use a Melles Griot 56 InGaAlAs laser (λ = 658 nm), a focusing lens and two etalons to generate a two-dimensional array of parallel laser beams. A 2-d array allows for inspection of wafer curvature uniformity and permits measurements of stress in two orthogonal directions if desired. Stress can be calculated in two directions provided that the corresponding moduli of the substrate are known. The laser is extremely stable over many hours, providing a near Gaussian shaped intensity distribution for all incident spots.

As shown in Figure 3 light is incident upon the backside of wafers, i.e., the side not facing the deposition flux. After reflecting off the backside of a substrate, the laser beams are directed to a high-speed CCD camera. A flat mirror having a wavefront distortion = 1/20th wave is used to reflect the light onto a 768 x 493 pixel detector. An extension tube attached to the camera prevents background light from entering the CCD. The camera can operate at high speeds including shutter opening times of 1/10,000 sec. High shutter speeds help reduce the effects of vibration and eliminate the effects of image blur from a moving substrate. The camera is operated in video mode when stationary samples are positioned directly under the viewport. Alternatively, an external device may trigger the camera to obtain an image of laser spots when substrates are rotated.

A 12-bit programmable shaft encoder triggers the CCD camera while samples are rotating. The rotary encoder is connected to a vacuum feedthrough that attaches to the spinning sample platen. Up to seven separate programmable trigger outputs are available that can accommodate any rotation speed. This encoder has 4096 counts per 360^{o} (an angular resolution of 0.087^{o} / count). The encoder count that corresponds to a centered substrate is recorded prior to each experiment and referenced throughout. Note, this count is different in static versus dynamic mode. A communication signal delay time is taken into account when samples are rotating to ensure that the same wafer area is monitored throughout an experiment.

A 500 MHz – clock speed computer controls the laser power, acquisition of images, and data calculations. The user interface offers control of laser power including automatic adjustment of laser intensity for varying surface reflectivity (not a requirement

in these experiments that direct light onto the backside of substrates). All data is updated continuously to real-time charts.

Analysis involves the determination of reflected laser spot centroid positions and calculation of spot spacings. Spot spacings determine curvature once an accurate measurement of the laser-sample-detector geometry is established. The initial spot spacings (a measure of curvature) must be determined by the MOSS instrument prior to an experiment to correctly interpret the changes that occur during thin film processing. The laser spot array typically covers a 5mm x 5mm area. Although this does not cover the entire wafer, average film stress can be determined quantitatively. Even though the curvature of a substrate is not constant across a wafer, the change in curvature developed during fabrication is similar provided that film thickness and the process conditions are constant at all points on a sample. For all experiments described herein, a 2 x 3 array (6 total beams) is used for analysis.

A video monitoring system is utilized to record optical images of thin film - substrate interfacial structure changes during reaction of Sc with deuterium and cooldown. This aids the understanding of changes in stress detected by MOSS. The optical imaging system consists of a high resolution CCD video camera attached to a long working distance, telescopic microscope with magnifying and focusing optics, as shown in Figure 4. The optical system is attached to a video monitor and videocassette recorder (VCR) to observe and record changes. The system shown in Figure 4 is mounted vertically on a 5 cm diameter boom, allowing radial movement. This is attached to a solid post fastened vertically to the top of the vacuum chamber at a flange hole. Visual changes at the substrate-film interface are obtained by focusing through a clear viewport positioned 120 degrees away from the laser viewport along the path of sample motion. Observations are made by viewing through the backside of a clear substrate; changes on cermet substrates cannot be probed with this setup.

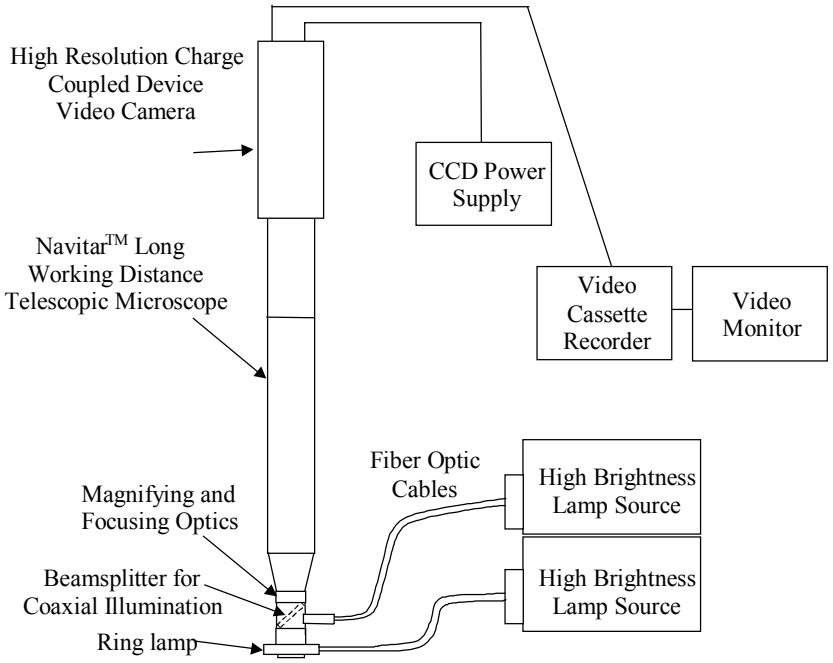

Figure 4 Optical microscope setup used to study changes in interface morphology and structure.

Two different high-brightness light sources, a ring lamp and a beamsplitter, are required to properly illuminate the sample at different stages of the fabrication process. Illumination effects are shown in Figure 5, where (a) demonstrates the effect of using a ring lamp and (b) shows the effect of a direct light through a beamsplitter for coaxial illumination. Imaging with a ring lamp highlights subtle structure at the metal – quartz substrate interface. The coaxial illumination is useful for viewing cracks that penetrate deeply through a film.

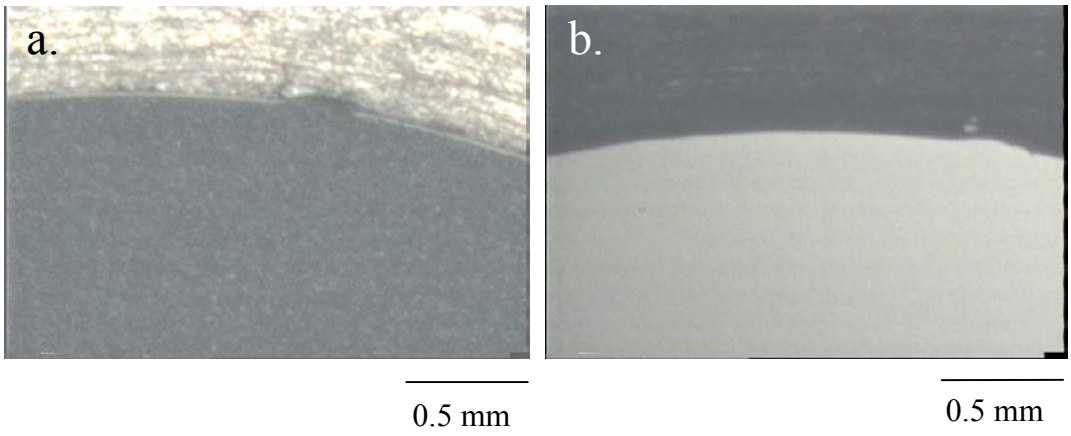

Figure 5. Illumination effects with ring lamp (a) and focused source with beamsplitter (b). Single film shown is ScD_2/Cr on quartz maintained at growth temperature. Subtle interface structure (not cracks) is present at this stage.

Section III. Substrate specifications and MOSS measurement sensitivity

Choice of substrates

In this work ScD_2 films with a thin Cr underlayer are deposited onto three different substrate materials in order to probe the influence of the starting surface and to research the properties of scandium dideuteride. Quartz and single crystal, α-Al_2O_3 (corundum) are useful for investigating the thermomechanical properties of films, for these two materials have different coefficients of thermal expansion. Molybdenum-alumina cermet is used for a third set of experiments because of its relevance for Defense Program applications.

For each wafer material, it is essential to choose a substrate thickness that permits a detailed study of stress. Not knowing the degree to which a wafer would bow during processing, it is necessary to iteratively fabricate a film onto a wafer having a particular thickness and change the wafer thickness for the following run accordingly. There are

several factors that influence the final wafer thickness. Most importantly the reflected spot array must remain on the camera throughout a process. Large tensile stresses are particularly important for the current geometry, since this leads to an increase in spot spacing. If wafer thicknesses are chosen too small, tensile stress can lead to the migration of a single spot or spots off the camera, thus ending the data acquisition prematurely. On the other hand, we desire to sensitively probe changes in curvature. This requires a small wafer thickness. In general, it is the tradeoff between these two factors that determines wafer thickness for experiments.

After conducting several preliminary tests we choose wafers having the following characteristics:

Material, Diameter	Source	Wafer Thickness, h_s,	Roughness, R_a, on Film Growth Side	Biaxial Modulus, M (GPa)
Quartz, 25 mm	Technical Glass, Inc.	650μm (0.026")	3.1 nm	87
Sapphire, R-plane (1$\underline{1}$02), 37 mm	Bicron-Saint/Gobain Crystal, Inc.	325μm (0.013")	300-350 nm	562*
Mo-alumina cermetCND50, 25 mm	Sandia National Laboratories	400μm (0.016")	40 nm	421 (ref. 9) 333 (nanoindentation)

* R-plane sapphire is not elastically isotropic in the plane of the film. The modulus specified for this substrate represents the value calculated from the Al_2O_3 stiffness tensor for the R-plane in a direction perpendicular to the wafer flat.

Table 1: Description of wafers.

Cermet wafers are fabricated at Sandia National Laboratories from cermet CND50 powder. CND50 cermet contains 50 wt% (27 vol%) Mo.[9]

Figure 6 shows a mold made from alumina (Sandi94) used to contain cermet during substrate fabrication. The molds used to create 25 mm diameter cermet wafers are made from isopressed alumina powder logs that are machined with a pocket on one side. After the pocket is filled with a cermet slurry, the blanks are oven dried at 120°C for 12 hours and then isopressed at 205 MPa ($3x10^4$psi). Cermet blanks are then machined and fired at 1650°C to achieve full densification. The outside diameter is

ground to 25 mm followed by a surface grind to remove the alumina mold material and isolate the cermet. Cermet blanks are then machined to a thickness of 625 μm.

Figure 6 Blank of cermet inside mold before firing at 1650°C.

The 25-mm diameter cermet disks are carefully lapped and polished sequentially to obtain a desired thickness of 400 μm. This is accomplished by double surface lapping with a 30 μm diamond water based slurry to a 450 μm thickness using cast iron plates. Next, the wafers are double-lapped using 15 μm diamond water based slurry with tin plates to a 400 μm thickness. The disks are then heated to 175°C and spaced evenly on a quartz crystal carrier at the same temperature with melted wax at the carrier edges. The hot quartz carrier with the disks and wax are placed on a level table with a weight on top and allowed to cool for one hour. A 1-μm diamond slurry is used with a nylon polishing cloth to polish the cermet and to remove the wax.

The Young's modulus of cermet wafers fabricated for this study is measured by nanoindentation and is equal to 250 GPa. For a Poisson's ratio of 0.25,[9] this gives a biaxial modulus of 333GPa.

Requirements of wafer backside polish for measurement of curvature

For all experiments in this study, wafer curvature is probed by directing light onto the back of substrates (side not receiving evaporation flux). Although either side of a

wafer can, in principle, be probed to determine curvature, this geometry is chosen because of accessibility. It is therefore essential to work with wafers that have polished, reflective backside surfaces. Sufficient reflected laser light intensity must reach the CCD camera detector for accurate measurement of curvature. Further, the intensity of each reflected laser spot must also be symmetric in shape and not distorted due to sample roughness or internal reflections.

Four hundred micron-thick cermet substrates are made with a sufficiently smooth backside for wafer curvature measurements. Polishing reduces the surface roughness to an acceptable level for curvature measurement. We determine the maximum allowable roughness, R_a, to be 40 nm (~1.6 microinch), as measured by a Dektak surface profilometer using a 12 μm-radius tip. Surface roughness greater than this value reduces the laser light intensity and leads to distorted spot shapes.

For semi-transparent substrate materials (quartz and sapphire), it is necessary to coat the backside with a reflective film. Although a small amount of laser light is reflected by virgin substrates, these wafers offer insufficient intensity for analysis with a 2-d array. We find that a 50-80 nm thick layer of chromium is sufficiently reflective. Cr layers are deposited by electron beam evaporation. Ideally the backside Cr layer should not affect the interpretation of data for ScD_2 growth. The minimal effects of a backside Cr layer are described in the next section.

Control experiments with semi-transparent substrates

Control experiments are performed to verify that Cr deposited onto the backside of sapphire and quartz wafers has a negligible effect on the curvature changes observed during ScD_2/Cr film processing. Potentially this backside layer could stress from heating, etc. and introduce an additional signature falsely attributed to ScD_2 growth.

For control experiments, sapphire and quartz wafers of previously listed thicknesses are coated with 50-80 nm Cr on the backside and subjected to conditions identical to that found during scandium dideuteride growth *except for* metal deposition. An experimental process flow diagram is shown in Figure 7. This plot summarizes the various fabrication steps involved with growth of ScD_2/Cr films and lists the techniques

used to probe stress and structure. Changes in temperature experienced during fabrication are also indicated qualitatively. This diagram fully depicts the steps involved with growth experiments described in latter sections. For control experiments, most of the same steps are used (heating, deuterium exposure, cooldown). However, we avoid depositing Sc/Cr films, since we desire to know solely the degree to which the backside layer is modified. For the control experiments, the electron beam evaporators are turned on for a period of time, but the shutters are kept closed. This procedure accounts for every source of heating except for condensation energy which probably has a negligible effect on the back surface layer.

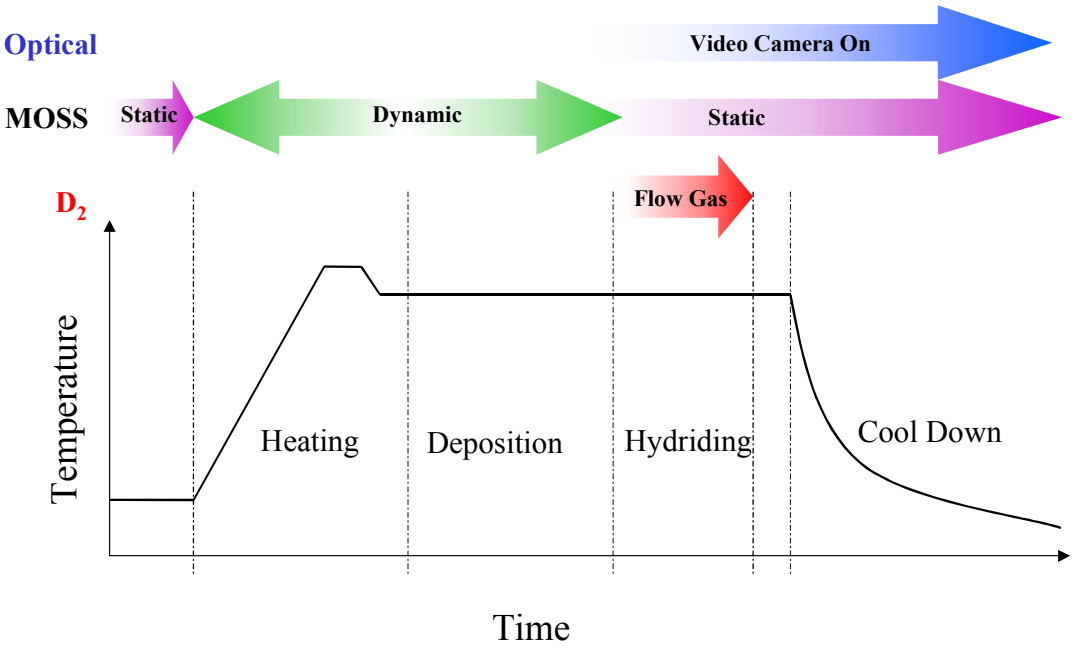

Figure 7 Process flow diagram for experiments. Also indicated are two techniques used to monitor stress and interface structure. 'Dynamic' refers to rotating samples; 'static' implies stationary substrates. Control experiments do not involve metal deposition.

As shown in Figures 8 and 9, minimal curvature changes are observed during control experiments. Figure 8 shows the results from a control experiment with sapphire, and Figure 9 displays data taken on quartz. The data shown in each figure is spliced together from several individual MOSS scans including

1. a baseline scan with the sample stationary and at T=30^{o}C
2. a scan taken with substrate maintained at an elevated temperature and rotating,

3. a measurement while the evaporators are turned on (shutters remain closed) and sample is rotating
4. a scan of curvature during D_2 exposure (sample hot and stationary)
5. a scan during cooldown (sample stationary)

For brevity we do not show the data taken when the sample temperature is increasing - a period of time ~ 1 hour between steps 1 and 2. There is minimal curvature change during

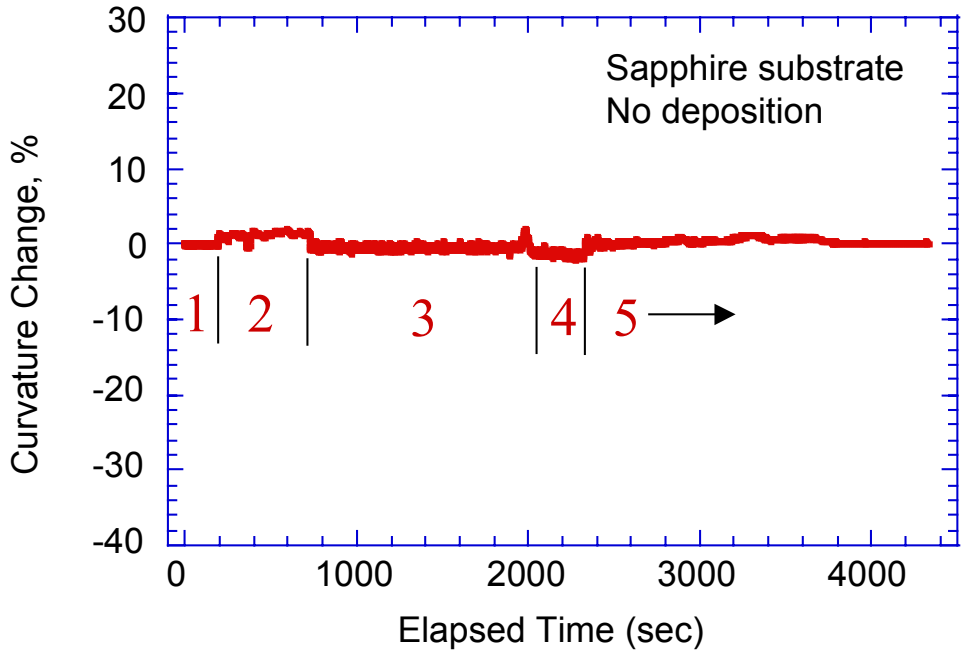

this temperature ramp as indicated by the close matching of scans 1 and 2.

Figure 8 Results from control experiment showing minimal sapphire wafer curvature changes during heating, D_2 exposure and cooldown. 'Wafer curvature' changes shown are actually MOSS laser spot spacing changes, $<\Delta D/D_o>$(%).

These control experiments therefore qualify Cr-backside coated quartz and sapphire substrates for measurement of stress evolution during ScD_2 layer growth. The subtle

changes in curvature shown in these plots are minute compared with the large changes described in the next section for growth of ScD_2.

The relatively smooth curves in Figures 8 and 9 also demonstrate success in

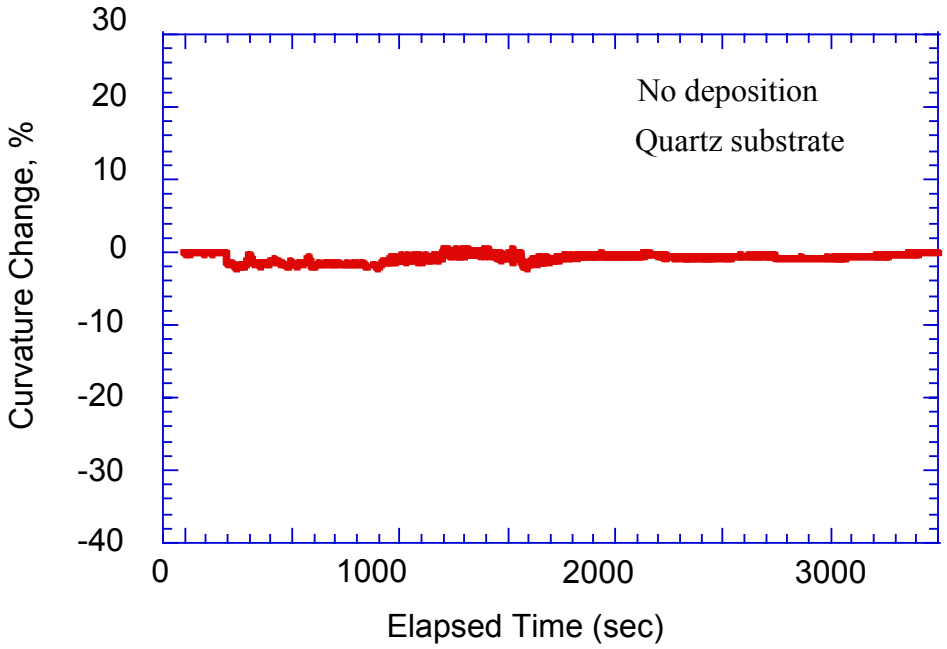

linking scans taken in static and dynamic modes. Careful determination of wafer position helps to ensure probing of identical locations on a sample during both operation modes.

Figure 9 Results from control experiment showing minimal quartz wafer curvature changes during heating, D_2 exposure and cooldown. 'Wafer curvature' changes shown are actually MOSS laser spot spacing changes, $<\Delta D/D_o>(\%)$.

MOSS sensitivity

The sensitivity in measuring curvature (and stress) for different modes of operation is also determined from Figures 8 and 9. The minimum resolvable curvature is calculated from the mean differential spot spacing $<\Delta D/D_o>$ observed for fixed temperature with no deposition flux impinging on a substrate. For this analysis, we take the mean differential spot spacing to be twice the standard deviation of the signal fluctuations. We spatially average over all measured spacings to calculate one mean spacing and hence one minimum resolvable curvature.

The highest sensitivity is found while samples are kept stationary and at low temperature. κ_{min} is approximately 0.0001 m^{-1} for a $<\Delta D/D_o>_{static}$ equal to 0.0002. Slightly decreased sensitivity is found at higher substrate temperatures. In dynamic mode, sample rotation leads to a lower sensitivity, approximately equal to 0.001 m^{-1}. Most likely platen eccentricity and wobble during spinning give rise to this higher noise level. All measurements are made with the vacuum system cryopump operating.

Section IV. ScD_2/Cr thin film growth experiments

Experiments investigate the development of stress and, when possible, interface structure during ScD_2/Cr thin film growth. Films are processed onto each of three substrate types, as described in separate sections. Each step of processing is analyzed including deposition, reaction with deuterium and cooldown (See Figure 7 for process flow). The procedure used for analyzing wafer curvature is the following.

Step 1 : Obtain measure of initial wafer curvature while sample is at 30^{o}C and stationary under the MOSS viewport. Curvature is probed for a minimum of 200 seconds to establish initial value.

Step 2 : With samples rotating and equilibrated at the growth temperature, probe curvature. For the first ~100 seconds, shutters cover the electron beam evaporators. Afterwards, shutters are opened and deposition begins. Films consist of a thin Cr layer and a thick Sc coating. After deposition, continue to probe curvature for a brief amount of time.

Step 3: Rotation of samples is stopped and the wafer used for probing stress is positioned directly under the viewport. (For experiments with quartz substrates, a second wafer is automatically positioned under a different viewport for optical imaging). Using video mode on the MOSS camera,

wafer curvature changes are probed as deuterium gas is introduced into the process chamber. This scan continues after the gas source valve is closed.

Step 4: With samples stationary, scan wafer curvature during cooldown to 30^{o}C. For quartz also monitor changes in witness sample optically.

For all experiments, we do not show the curvature data taken during the temperature ramp prior to deposition, because zero $\Delta\kappa$ is observed. The curvature measured during step 1 (sample at 30^{o}C, stationary) matches closely to that measured during the initial stages of step 2 (sample at growth temperature and rotating).

ScD_2 /Cr films processed on sapphire substrates

Growth of metal hydride thin films onto several sapphire wafers is investigated. Sapphire substrates are initially cleaned using a solvent rinse and baked in the growth system at 200^{o}C for several hours and at 525^{o}C for 5 minutes. After cooldown to ~30^{o}C, each substrate is measured to determine initial curvature represented by a zero mean differential spot spacing in Figure 10. This does not imply that a wafer is perfectly flat initially (radius of curvature infinitely large). However, it is a reference for changes in curvature that develop during processing. Changes in curvature are required to determine stress state or quantify stress when using the laser-based technique.

As shown in Figure 10 large changes in film stress develop during processing onto sapphire. The data indicates no significant sapphire wafer curvature change during metal deposition (step 2). A minimal curvature change during this stage is indicative of near-zero growth stress. We expect that the film develops a finite intrinsic stress during deposition; yet, compared with the large stress changes observed in steps 3 and 4, it remains undetected when using 325 μm thick sapphire. A large change in stress is, however, observed during deuterium exposure at fixed, elevated temperature. This is demonstrated in Figure 10, step 3. The initial part of step 3 is unchanged, because this is

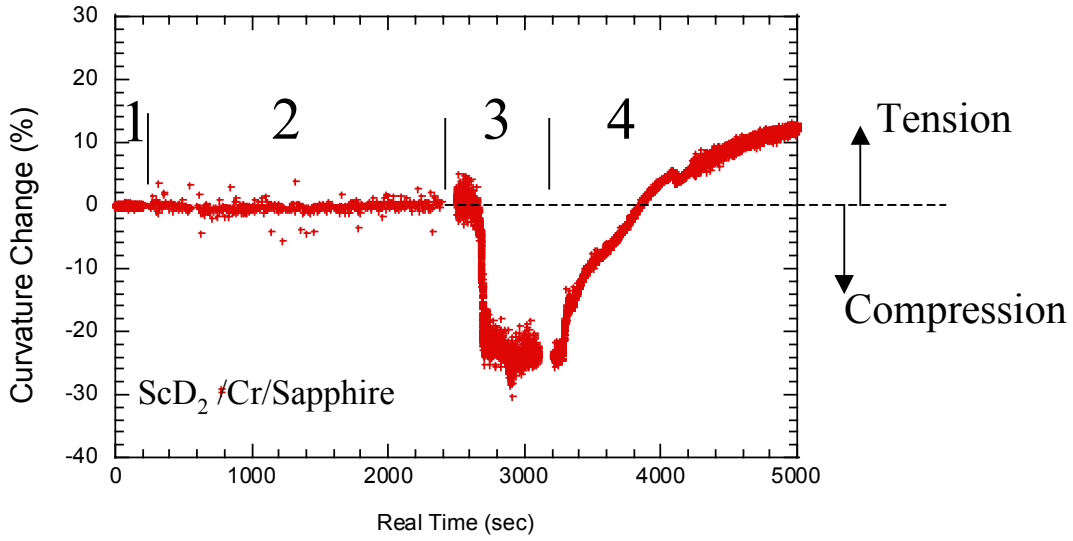

Figure 10 Changes in sapphire wafer curvature during thin film fabrication process including depositions (step 2), reaction with D_2 (step 3) and cooldown (step 4). 'Wafer curvature' changes shown are actually MOSS laser spot spacing changes, $<\Delta D/D_o>(\%)$.

time prior to gas introduction. Almost immediately after introducing deuterium into the chamber, a change in wafer curvature is observed corresponding to a compressive film stress (negative ordinate value on graph). The film maintains a large compressive stress even after the reaction is complete. We expect that the predominantly flat portion of the curve in step 3 (between 2700 and 3100 sec) corresponds to the time after complete transformation to a dideuteride phase. Deuterium gas remains in the chamber during this period, yet no curvature changes are observed. The development of a compressive stress is expected upon reaction due to a change in composition. As-deposited Sc metal is initially constrained to the substrate by adhesion. The reaction of metal with deuterium increases the atomic density and eventually changes the phase of the film.

A closer look at the wafer curvature changes during deuterium exposure reveals several other trends in stress development. In Figure 11 we show a portion of the Figure 10 plot that displays the period of time corresponding to deuterium introduction and

reaction. After deuterium is introduced (indicated by an arrow), there is a sudden buildup of compressive stress. The initial increase in compression occurs up to a level indicated by a mean differential spot spacing change $<\Delta D/D_o> = -24\%$. After this, the film temporarily develops a lower compressive stress and then returns to a higher stress value. We refer to this trend as a 'double reversal' in stress. Possible explanations for this behavior are presented in Section V.

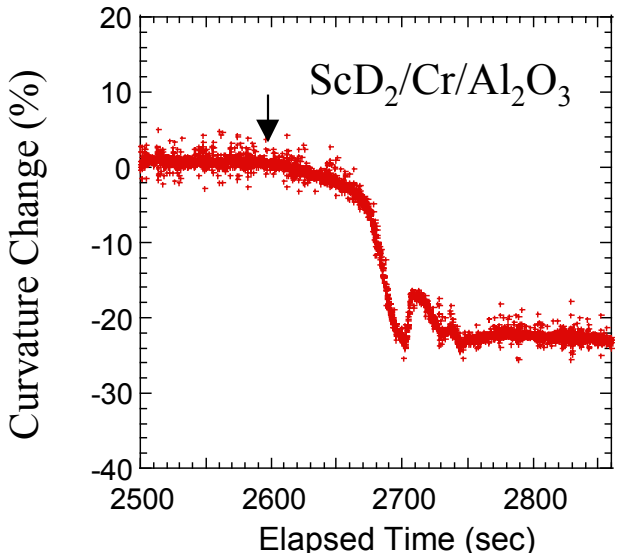

Figure 11 Plot of sapphire wafer curvature changes during reaction of Sc layer. 'Wafer curvature' changes shown are actually MOSS laser spot spacing changes, $<\Delta D/D_o>(\%)$.

After hydriding, the heaters are turned off, and the sample is cooled. During cooldown, the film transitions to a tensile stress state indicated by a positive ordinate value in Figure 10, step 4. A tensile stress originates from the mismatch in thermal expansion coefficients between the ScD_2 film and sapphire substrate. As a sample is cooled, the film lattice contracts at a greater rate than the underlying substrate. No evidence of stress relief during cooldown is detected for experiments with sapphire. This is consistent with the continuously increasing wafer curvature shown in step 4. Note, the three small displacements in Figure 10, step 4 are the result of manual adjustments to the MOSS mirror orientation. This is occasionally required to keep the reflected beams on

the CCD camera; slight platen bending occurs during a temperature change resulting in a small deflection of the beam array.

ScD_2 /Cr films processed on quartz substrates

In several respects the evolution of stress in films deposited onto quartz is similar to that developed for growth onto sapphire. As summarized in Figure 12, almost no intrinsic stress is observed during metal deposition. This includes growth of a thin Cr layer followed by a thick Sc film. Hydriding again leads to a large compressive stress which can be expected based on changes in atomic density. Scandium dideuteride films

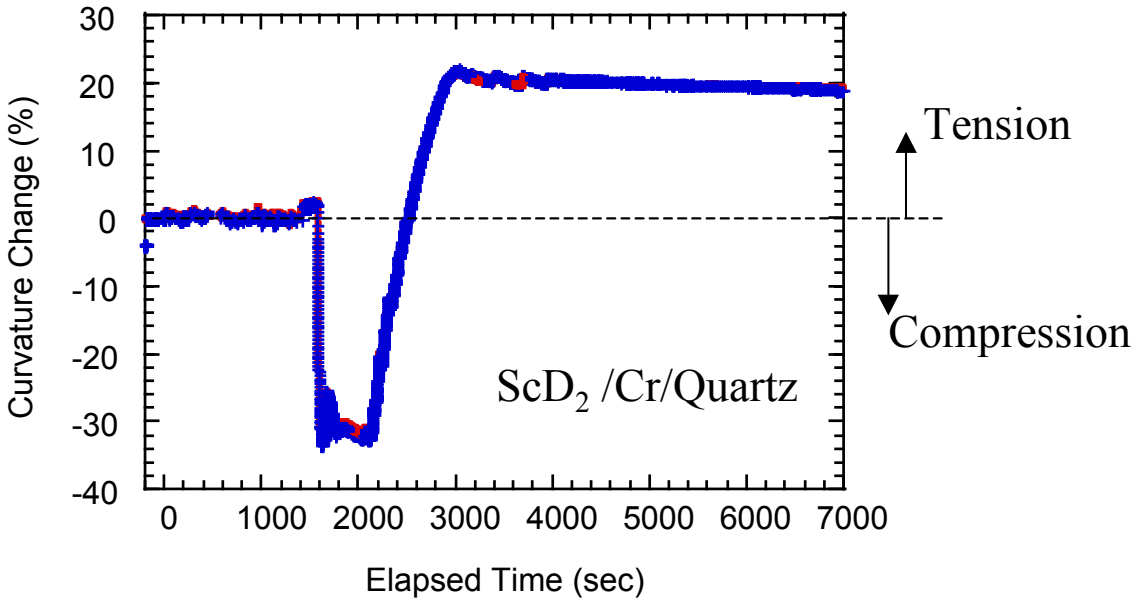

Figure 12 Changes in quartz 'wafer curvature' during processing of ScD_2 / Cr thin films. 'Wafer curvature' changes shown are actually MOSS laser spot spacing changes.

remain in compression at the growth temperature. A 'double reversal' in compression again characterizes the apparent latter stages of chemical reaction as shown in Figure 13.

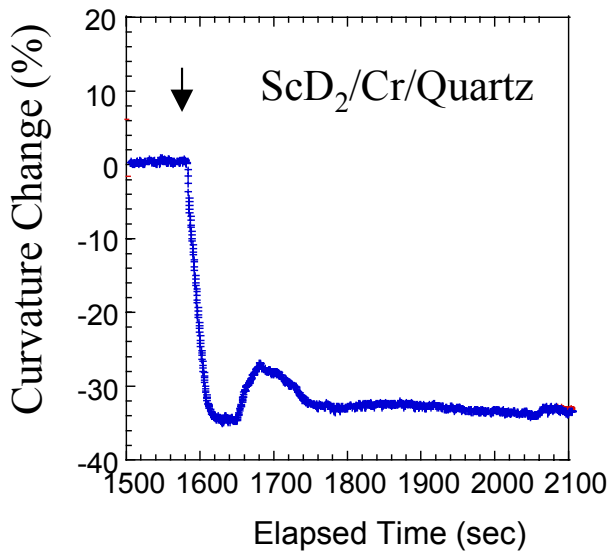

Figure 13 Plot of quartz wafer curvature changes during reaction of Sc layer. 'Wafer curvature' changes shown are actually MOSS laser spot spacing changes, $<\Delta D/D_o>(\%)$.

Films deposited on quartz exhibit very different behavior during cooldown compared with sapphire. As the temperature is decreased, films again develop a large tensile stress due to the difference in thermal expansion coefficients (CTE of quartz = 5.5×10^{-7} /°C). However, at a temperature of approximately 250°C during cooldown, there is evidence of stress relaxation. In Figure 12, relief begins at time 2950 sec. Once cooled to 30°C, the stress state of the film is tensile.

The stress relief during cooldown detected by the wafer curvature sensor is correlated with a transition in film structure. In general, cracks nucleate and grow once the extrinsic stress becomes sufficiently large. Crack formation is observed on a second quartz witness sample (not having Cr on the wafer backside) when using the optical microscope apparatus. This second quartz wafer is positioned so that a large area of the film - substrate interface can be observed. At approximately 250°C during cooldown, the film fractures into large fragments as demonstrated in Figure 14.b. As the sample continues to cool, the large fragments instantaneously break into smaller fragments. The arrows in Figure 14 b. and c. point to the same region where an instantaneous fracture

occurred with large fragments remaining on either side. Fracture appears to end at T~150°C.

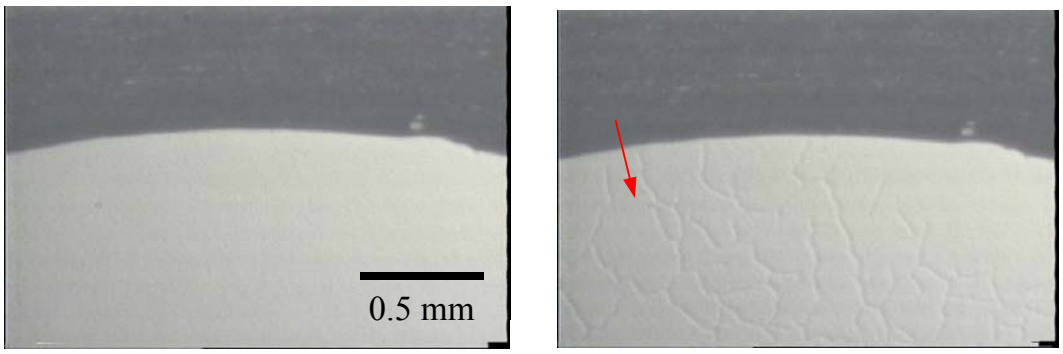

(a) Film at the reaction temperature (b) Initial fracture during cooldown.

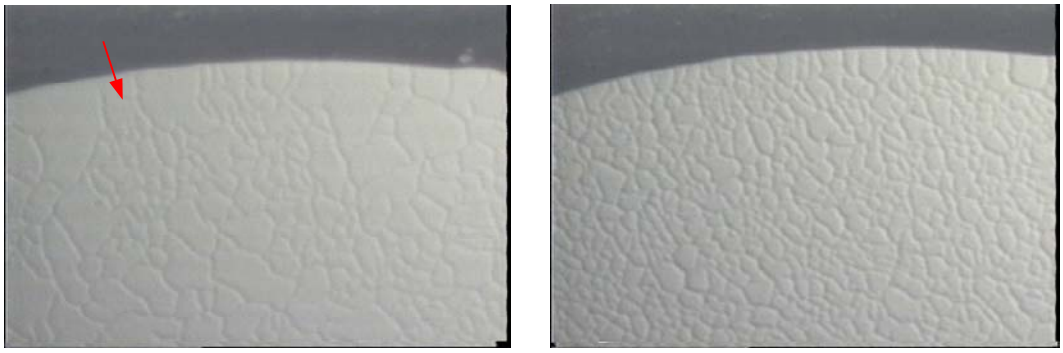

(c.) Interim large and small fragments. (d) Final visual state of film-substrate interface.

Figure 14 Optical micrographs showing substrate - film interface during cooldown from the reaction temperature. Cracks nucleate and grow as the temperature decreases.

ScD_2/Cr films processed on cermet substrates

Two sets of experiments investigate stress evolution for films deposited onto molybdenum – alumina cermet wafers. In the first, cermet wafers are solvent cleaned and vacuum baked at 200° and 525°C in the deposition system. In the second set of experiments, cermet wafers are again solvent cleaned, and the surface is sputter cleaned using 1200eV Ar^+ ions at ~30° incidence angle in a separate vacuum system. These samples are also baked as above in the deposition system prior to growth. Previous work

by Goeke and Romero demonstrates that Ar^+ ion sputtering removes a loosely bound particulate layer that remains from mechanical polishing. This should improve film adhesion, and potentially affects film stress. All cermet wafers are fabricated from CND50 powder using the procedure described in Section III. These substrates consist of 50 wt% (27 vol%) Mo and are 400 μm thick.

ScD_2/Cr films fabricated onto cermet substrates exhibit large compressive and tensile stresses during processing, regardless of the cleaning procedure. Figure 15 summarizes the curvature changes developed during growth of films onto solvent

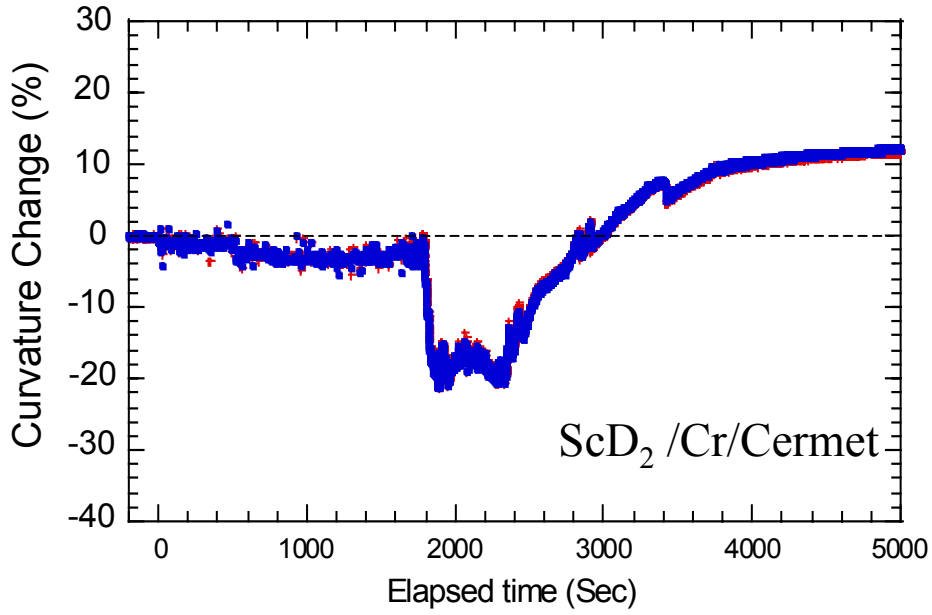

Figure 15 Plot of cermet wafer curvature vs. time for entire thin film fabrication process. 'Wafer curvature' changes shown are actually MOSS laser spot spacing changes, $<\Delta D/D_o>(\%)$.

cleaned, vacuum baked wafers. Figure 16 plots the evolution of curvature when films are deposited onto wafers pre-treated with an Ar^+ ion beam. No intrinsic stress is observed during metal deposition in both cases. The stress developed during metal deposition is small compared with the large compressive stress developed during reaction with deuterium. A compressive stress develops, because the initially well-adhered scandium

film changes atomic density then phase. Films deposited onto cermet substrates also show a 'double-reversal' in compression towards the apparent end of hydriding.

A tensile stress develops during cooldown, and the films remain in tension as the temperature approaches 30°C. This indicates that scandium dideuteride films have a greater thermal expansion coefficient than the cermet. The tensile stress developed

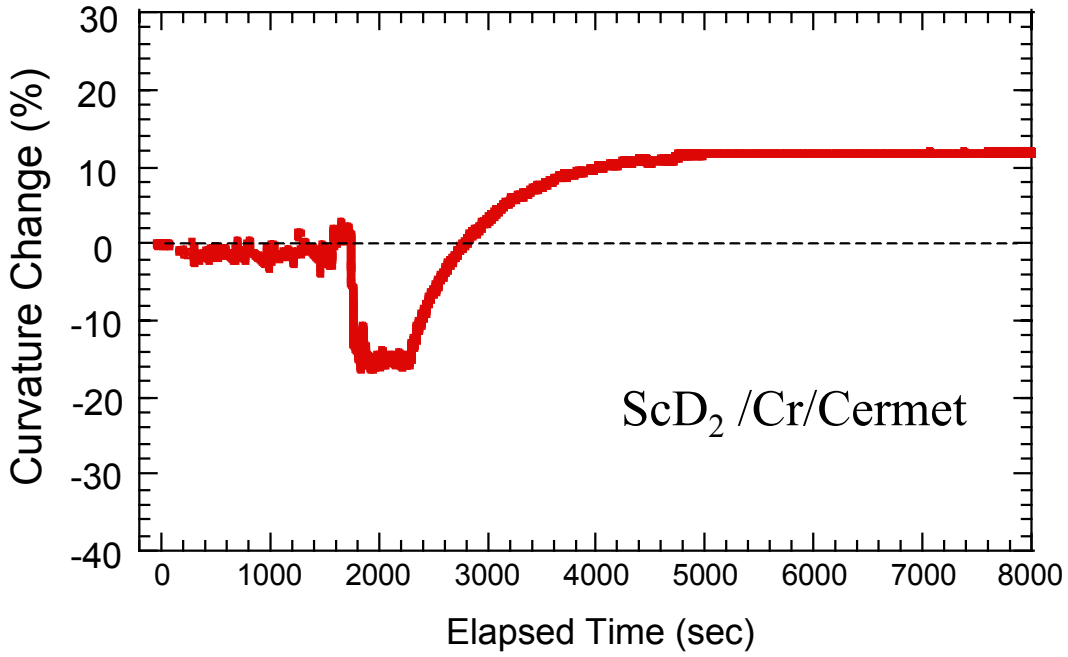

Figure 16 Plot of cermet wafer curvature changes vs. time. Cermet wafer is ion beam cleaned ex-situ prior to film growth. 'Wafer curvature' changes shown are actually MOSS laser spot spacing changes, $<\Delta D/D_o>(\%)$.

during cooling is not sufficient to generate cracks similar to those seen on quartz. In fact, no stress relief is observed in films grown onto this lot of cermet wafers, as indicated by a continuously increasing wafer curvature, Figures 15 and 16. Note, the three small displacements in curvature shown in Figure 15 during the cooldown portion are artifacts resulting from manual adjustments of the MOSS mirror orientation.

Section V: Discussion of stress changes during reaction with deuterium– all substrate materials

The net compressive stress developed during hydriding can be understood by an increased atomic density compared with the as-deposited scandium film. The scandium layer is initially deposited with relatively little stress, and it can expand or contract out of the plane of growth upon reaction with deuterium gas. However, because it is well adhered to a substrate, reaction to form ScD_2 generates an in-plane, compressive stress.

Additional work is needed to understand subtle stress changes observed during the latter stages of hydriding. In particular, a 'double reversal' in compression is observed in each experiment for all three substrate materials.

We presently consider several possible explanations for this behavior, including changes in film or interface structure. It is possible that films plastically deform during reaction with deuterium. The formation of defects, such as dislocations, may affect curvature although additional electron microscopy is required to confirm that changes in microstructure (defect density) occur. Alternatively, films may buckle from substrates during reaction with deuterium. Large amounts of compressive stress can induce delamination locally.

Evidence of structural transformations at the substrate – film interface during chemical reaction with deuterium is shown by optical microscopy. Viewing through a second quartz witness sample that is not coated with Cr on the backside shows localized changes in reflectivity (see Figure 17). The darker region is the substrate-film interface (a) prior to, and (b) after deuterium dosing. During the initial introduction of deuterium into the chamber, the substrate – film interface remains smooth and highly reflective with a very dark appearance. As deuterium continues to fill the chamber, the interface gradually develops a high density of light scatter centers. The point-like features may be localized sites of delamination.

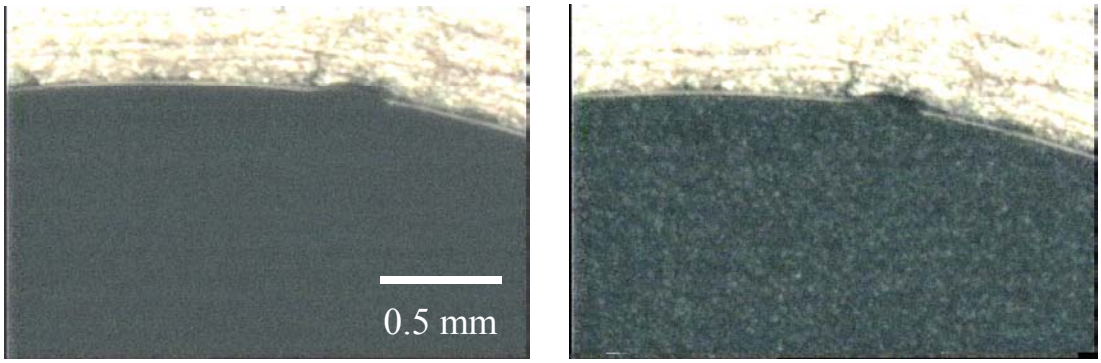

Figure 17 Thin film changes, (left) prior to, and (right) after introducing deuterium. Images show interface structure of films deposited onto quartz. Images are acquired by viewing through a wafer.

Interestingly, separation along ScD_2-Cr or Cr-substrate interfaces as a result of a high compressive stress is not detected after removing films from the deposition system. Films grown on quartz substrates are extracted from the growth apparatus and then cross-sectioned in predetermined areas using a focused Ga ion beam. Afterwards, the sample is placed in a scanning electron microscope to probe the interface and layer structure covering many thousands of μm^2 in area. Scanning electron microscopy shows no evidence of blisters or buckles at the substrate-Cr or Cr-ScD_2 interfaces as demonstrated in Figure 18. In all cases, films grown onto quartz substrates only show cracks that are nonplanar with respect to the substrate. Still, it is possible that films buckle during reaction with D_2, but exhibit no delamination after removal from the vacuum system. The generation of tensile stresses during cooldown could cause buckled areas to return to their original planar morphology thus masking their detection. Additional analysis of films grown on sapphire substrates that show no cracking should elucidate the presence/absence of blisters.

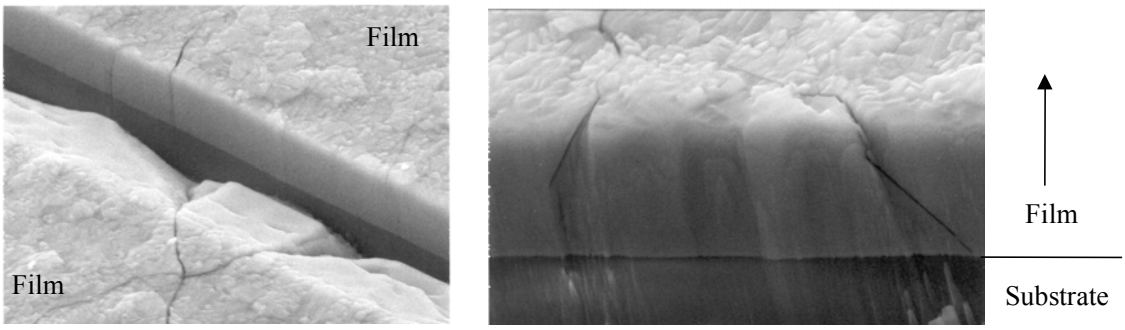

Figure 18 ScD_2/Cr thin film grown onto a quartz substrate. Predetermined area has been cross-sectioned by focused gallium ion beam sputtering. Image reveals cracks in thin film penetrating to substrate – film interface.

In addition to plasticity and decohesion, it is also plausible that the stress developed during hydriding (specifically the 'double reversal') is affected by a gradual phase transformation. A net compressive stress is expected upon hydriding due to a change in density. However, the transformation of a hexagonal Sc lattice to a cubic ScD_2 phase involves several distinct steps. Each of these could give rise to a change in stress.

According to Sc-D thermodynamic phase diagrams[10], initial loading of films results in a solid solution of deuterium in scandium. Deuterium populates tetrahedral interstices within the hexagonal Sc lattice during this time,[11-13] and the change in density corresponding to this compositional difference should result in a continuous buildup of compressive stress if no other modifications to microstructure are induced. This would correspond to the initial rise in compression detected by MOSS. After a large number of interstices are filled, the dideuteride phase nucleates. Beginning at a relatively large deuterium composition of ~32 at.%, two distinct phases coexist for a period of time, including the hexagonal α–Sc phase and the cubic scandium dideuteride lattice. The presence of two phases should affect film stress, and, potentially, this leads to a temporary reduction in compression (corresponding to the first reversal). The two-phase

film continues to exist until a composition of $ScD_{1.6}$ is reached, assuming no variation through the thickness. With continued dosing the entire layer is converted to the cubic phase. It is expected that the continued loading of single-phase $ScD_{1.6}$ to stoichiometric ScD_2 would again correlate with a continuous buildup of compressive stress. The crystal structure of the film is identical during this latter stage, and the layer is only changing density.

Assuming that ScD_2/ Cr films remain completely attached to substrates during reaction with deuterium, it is possible to estimate the final compressive stress attained. The stress is calculated using Stoney's formula expressed as

$$\sigma = \left(\frac{M_s h_{s\,2}}{-6h_f} \right) * (\kappa - \kappa_o) \qquad (1)$$

with M_s = biaxial modulus of substrate, h_s = thickness of substrate and h_f = thickness of film. Although the Sc thickness is fairly large it is still a small percentage of the wafer thicknesses used, and therefore Stoney's formulation is accurate. For MOSS measurements the curvature is related to the measured spot spacing changes and the laser-substrate-detector geometry by

$$D\text{-}D_o/D_o = 2L\kappa/\cos\,\alpha \qquad (2)$$

with L = distance from substrate to detector, α = angle of laser light incidence, D = final spot spacing and D_o = initial spot spacing.

The compressive stress attained during reaction with deuterium is listed in Table 2 for the three substrate materials. These are expressed in terms of the final film thickness, $h_{f(1x)}$, in microns. It is this same '1x' thickness that is used in the calculation of stress via Stoney's formulation despite the use of a two-step growth process.

In general, the maximum stress developed during reaction is similar for growth on all three substrate materials. Although the observed changes in curvature are very different, taking into account the different wafer thicknesses and stiffnesses reveals near-

identical values for stress. Note, the moduli used for quartz and cermet are average values. Thus, the error associated with these two calculated values is larger than that for films grown on single crystal sapphire for which the modulus is known precisely.

Substrate Material	Biaxial Modulus, M (GPa)	$M(h_s)^2$ Product (GPa-μm^2)	Laser spot spacing change $<\Delta D/D_o>$ (%)	Maximum compressive stress developed during reaction with deuterium (GPa)
Quartz	87	3.68×10^7	35	$1.35 / h_{f(1x)}$
Sapphire	562	5.94×10^7	24	$1.50 / h_{f(1x)}$
Cermet	421 (ref. 9) 333 (nanoindentation)	6.74×10^7 5.33×10^7	18	$1.28 / h_{f(1x)}$ $1.01 / h_{f(1x)}$

Table 2 Laser spot spacing changes and corresponding maximum compressive stress attained during reaction with deuterium. h_f is expressed in microns.

Section VI: Thermomechanical properties of scandium dideuteride thin films

The development of tensile stress during cooldown occurs because of a mismatch in thermal expansion coefficients between substrate and film. Assuming that films are completely attached to substrates after reaction with deuterium, we are able to determine the coefficient of thermal expansion for ScD_2.

The stress change with temperature in the elastic range is governed by the following equation:

$$\frac{d\sigma}{dT} = M_f * (\alpha_s - \alpha_f) \qquad (3)$$

where

$\frac{d\sigma}{dT}$ is the derivative of stress versus temperature

M_f is the biaxial modulus of the film (for isotropically elastic material = $E/1-\nu$)

α_s is the substrate thermal expansion coefficient

α_f is the film thermal expansion coefficient

The α_s's are known for each of the substrate materials as listed in Table 3. These values are average coefficients taken over the range of temperatures between the growth temperature and 150°C.

Substrate Material	CTE of substrate, α_s ($x10^{-6}/^oC$)	Reference:	Slope of stress-temperature plot (MPa/°C)	CTE of ScD_2 film, α_f ($x10^{-6}/^oC$)
Quartz	0.55	[14] Technical Glass, Inc.	3.81	15.79
Sapphire	7.70	[15] Bicron,Inc.	2.10	16.10
Cermet	7.39	[9] S.J. Glass	2.07 (M_s=421 GPa) 1.64 (M_s=333GPa)	15.69 (M_s=421 GPa) 13.96 (M_s=333GPa)

Table 3 Coefficient of thermal expansion (CTE) for substrates and ScD_2 films. Values listed for ScD_2 films on cermet wafers are calculated using a modulus (421GPa) from reference 9 and a value determined by nanoindentation (333GPa).

Using the listed values for α_s and the slopes of the data plotted in Figure 19 we extract a measure of $\alpha_f|_{ScD2}$. This determines $\alpha_f|_{ScD2}$ to be15 x $10^{-6}/^oC$. Note, this is in good agreement with previous measurements by Lundin et. al.[16] The CTE, $\alpha_f|_{ScD2}$, was shown by Lundin to be 14.51 x $10^{-6}/^oC$ at 250°C. The CTE values calculated for individual experiments are also listed in Table 3, according to wafer type. For growth on quartz, we only consider curvature data for T > 250°C; this precludes the onset of cracking. Note, measurements after cracking are invalid because the film is no longer continuous. For these determinations we also ignore the effects of Cr underlayers, since

these films are much thinner than the ScD_2. For these calculations we set M_f =250 GPa as determined previously by nanoindentation.[1] A single average biaxial modulus is used assuming that the film is elastically isotropic in the plane of the wafer. An example of an isotropic film is one having a random in-plane texture.

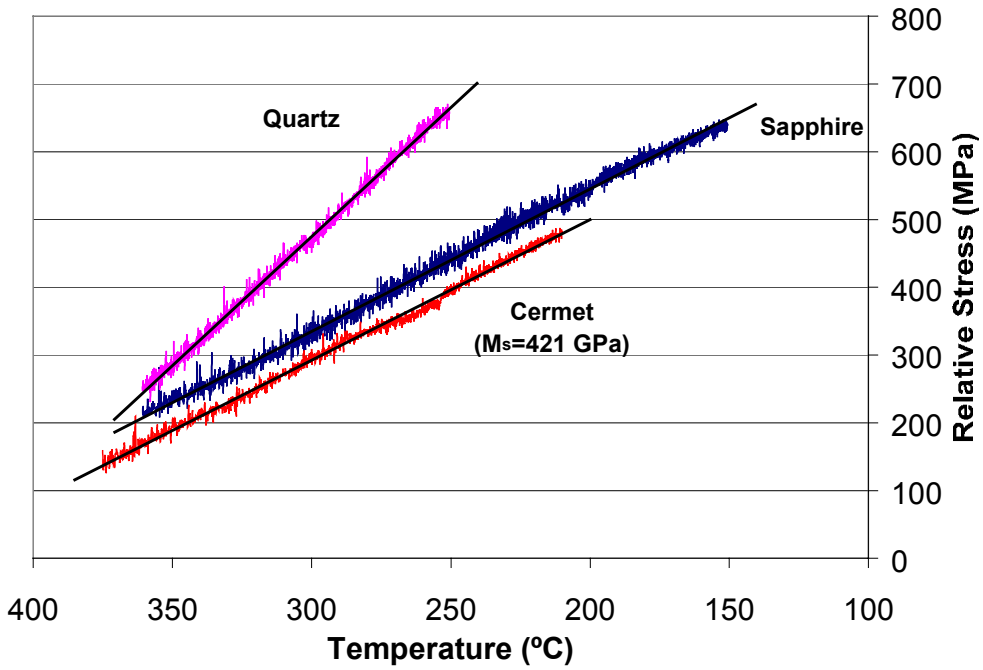

Figure 19 Plot of stress versus temperature during cooldown from the growth temperature.

Section VII: Conclusions and suggestions for future work

The evolution of stress in ScD_2 films having a thin Cr underlayer is determined for each stage of fabrication including metal deposition via evaporation, reaction with deuterium and cooldown. In general, large compressive and tensile stresses develops during fabrication. The net compressive stress generated during reaction with deuterium is explained by an increased atomic density compared with the as-deposited, low stress Sc thin film. A continuous buildup of compressive stress occurs during the initial stages of deuterium reaction, but 'stress relief' occurs during the latter stages. After fully

transforming to ScD_2, films remain in compression at the growth temperature. After reaction, films are cooled, and a tensile stress develops due to the mismatch in thermal expansion coefficients of the substrate-film couple. Films remain in a state of tension once cooled to 30°C.

The residual film stress and the propensity for films to crack during cooldown depends principally on the substrate material when using identical process parameters. Films deposited onto quartz substrates show evidence of stress relief during cooldown; this is correlated with crack nucleation and propagation within films. Films deposited onto cermet and sapphire substrates exhibit no stress relief during cooldown. The coefficient of thermal expansion of scandium dideuteride is measured to be 15×10^{-6} $^{o}C^{-1}$.

The techniques developed to probe film stress demonstrate the usefulness of the optical stress sensor for a manufacturing environment. The ability to quantitatively probe film stress while samples are rotating or stationary improves the flexibility of this technique. In this set of experiments, laser light is reflected off the backside of substrates, thus enhancing its functionality for a variety of settings. Cermet substrates of interest for DP applications are made sufficiently reflective by sequential polishing with fine diamond slurries. The addition of a backside Cr layer to semitransparent quartz and sapphire substrates allow precise measurement of curvature for these additional wafer materials. All are considered useful as witness samples in a production environment.

Application of MOSS technology to production systems

The potential application and implementation of a multi-beam, optical stress sensor to production equipment are examined in the following paragraphs.

Current production of ScD_2 films does not allow for film characterization during deposition and loading. This could lead to undesired process variables that remain undetected, resulting in the loss of expensive product. *In-situ* monitoring procedures for real-time process control would provide a means to evaluate deposition parameters and potentially prevent loss of product. Evaluation of the stress developed in a witness

sample should provide immediate feedback as to the state of films grown within a particular run.

The multi-beam optical stress sensor retrofitted to current equipment would provide such a process control technique for monitoring film stress during fabrication. When retrofitting existing systems for new equipment, the current configuration must be accommodated. Present deposition systems comprise a hemispherical substrate holder surrounded by removable shielding (see Figure 20). To incorporate the MOSS an additional port must be added to the top flange at an angle that will allow laser spot impingement to substrates. With regards to the MOSS system it is recommended to maintain perpendicularity to the sample, and it is critical to have an unobstructed line of sight view. This, however, is a trivial addition and a conceptual arrangement is illustrated in Figure 20.b. Only a slight modification to the top plate flange must be made. It is recommended that this viewport have a minimum glass diameter of 3.8 cm.

Figure 20: Schematic of deposition system used for processing of ScD_2 films is shown on left. Image on right shows same system with proposed addition of stress sensor.

There are several possible improvements to current MOSS systems. Collected data includes laser spot centroid spacings measured as the radius of curvature of a substrate changes. A complication arises when spots drift out of frame due to large curvature changes necessitating mirror adjustments to correct for the drift. Mirror adjustments are made manually at this time. Improvements to this analysis technique would consist of automatic control of mirror orientation. Mirror adjustments to maintain spot positions on the CCD camera array can be made by several methods among which are servo motors or piezoelectric actuators. Of these two piezoelectric options would be the most applicable. This is based on the restrictions imposed by vibration suppression and positioning accuracy. In conjunction with a personal computer and centroid location feedback an accurate positioning system could be devised. Commercially available software such as LabVIEW could be used to provide this type of control. Data reduction and presentation could be integrated into a LabVIEW package as well. Based on the suggestions of the authors, k-space Associates, Inc. is currently developing the auto-adjust mirror rotation feature for future MOSS models.

From the equipment integration and data reduction standpoint, a real time film stress monitoring system suitable for production could be fabricated with off-the-shelf parts and software. An easily understood 'visual indicator of product status' could be developed enabling equipment operators to take action if readings approach process control limits. Cost of system conversion would also be reasonable when taking into consideration labor and material investment loss due to a non-conforming lot of product.

Acknowledgements:

The authors value the efforts of T. Buchheit for help in determining cermet and sapphire substrate modulus, J. Floro for discussions of the stress sensor and film properties, M.B. Ritchey for SEM, D. Van Ornum and A. Charley for fabricating cermet substrates, and J. Cornejo for vacuum fixture cleaning. This work was performed at Sandia National Laboratories and is supported by the United States Department of Energy under Contract

No. DE-AC04-94AL85000. Sandia is a multiprogram laboratory operated by Sandia Corporation, a Lockheed Martin Company, for the United States Department of Energy.

References:

[1] David Lavan, Mike Eatough, Sandia National Laboratories, private communication, 2000.

[2] W.D. Nix, *Mechanical Properties of Thin Films*, Metallurgical Transactions A, **20A**, 2230-2231 (1989).

[3] D.P. Adams, L. Parfitt, J.C. Bilello, S.M. Yalisove, and Z.U. Rek, *Microstructure and Residual Stress of Very Thin Mo Films*, Thin Solid Films, **266**, 52 (1995). J. Tao, D. Adams, S.M. Yalisove, and J.C. Bilello, *The Origin of Anomolous Strain in Thin Sputtered Mo films on Si(001),* Mat. Res. Soc. Symp. Proc. **239**, 57 (1992).

[4] E. Chason, J.A. Floro, J. Reno, J. Klem, *Final Report on LDRD Project: In Situ Determination of Composition and Strain During MBE*, SAND report, SAND97-0295, (1997).

[5] G. Stoney, Proc. R. Soc. London, Ser. A **82**, 172 (1909).

[6] J.A. Floro, E. Chason, S.R. Lee, and G.A. Peterson, *Biaxial moduli of coherent $Si_{1-x}Ge_x$ films on Si(001)*, Appl. Phys. Lett. **71,** 1694 (1997).[7] S. Hearne, E. Chason, J. Han, J.A. Floro, J. Figiel, J. Hunter, H. Amano, I.S.T. Tsong, *Stress Evolution during Metalorganic Chemical Vapor Deposition of GaN*, Appl. Phys. Lett. **74**, 356-358 (1999).

[8] D.P. Adams, N. Moody, J.A. Romero, J. Floro, M. Rodriguez, *Development of Microstructure and Stress in Ion Beam Sputtered Erbium Hydride Thin Films*, MRS Proceeding, Spring Symposium, in press (2001).

[9] S. Jill Glass *et al* , *Mo-Al_2O_3 Cermet Research and Development*, SAND report, SAND97-1894, (1997).

[10] F.D. Manchester and J.M. Pitre, *The H-Sc (Hydrogen-Scandium) System*, Journal of Phase Equilibria, **18**, 194-204 (1997).

[11] A. Pebler and W.E. Wallace, *Crystal Structures of some Lanthanide Hydrides*, J. Phys. Chem. **66**, 148-151 (1962).

[12] W.M. Mueller, J.P. Blackledge, and G.G. Libowitz, *Metal Hydrides* (Academic Press, New York, NY) Ch. 10 (1968).

[13] C.E. Lundin (University of Denver), *The Structural and Thermodynamic Properties of the Sc-H System*, SAND Report, SCCR 72-3158, (1972).

[14] Technical Glass, Inc. (commercial vendor of substrates, 2000).

[15] Bicron-Saint/Gobain Crystal, Inc. (commercial vendor of substrates, 2000).

[16] C.E. Lundin (University of Denver), *Phase I: Structural study of Metal-Hydrogen System*, SAND Report, SCCR 70-6067, p. 32 (1970).

Distribution List:

L. Beavis (Dept. 14405, MS 0871)
J. Brainard (Dept. 02564, MS 0516)
C. Busick (Dept. 02564, MS 0516)
G. Laughlin (Dept. 02564, MS 0516)
M. Eatough (Dept. 01822, MS 1411)
W. Wampler (Dept. 01111, MS 1056)
D. Blankenship (Dept. 14405, MS 0871)
G. Smith (Dept. 02564, MS 0516)
N. Lapetina (Dept. 14405, MS 0871)
P. Miller (Dept. 01118, MS 1423)
J. Floro (Dept. 01114, MS 1415)
J. L. Provo (Dept. 14402, MS 0869)
W. Conley (Dept. 14405-1, MS 0871)
R. Poole (Dept. 14171, MS 0959)
R. Koss (Dept. 02564, MS 0516)
N. Demeza (Dept. 14100, MS 0960)
C. Adkins (Dept.14101, MS 0961)
F. Bacon (Dept. 02502, MS 0521)
F. Gerstle (Dept.16000 MS 0839)
L. Pope (Dept. 14405, MS 0871)
D. Malbrough (Dept. 14404, MS 0873)
B. Welberry (Dept. 14402, MS 0869)
L. Brown (Dept. 14171, MS 0959)
B. Silva (Dept. 14171, MS 0959)
J. Romero (Dept. 14171, MS 0959)
R. Goeke, 2 copies (Dept. 14171, MS 0959)
D.P. Adams, 2 copies (Dept. 14171, MS 0959)

Central Technical Files, (Dept. 08945-1, MS 9018)
Technical Library, 2 copies (Dept. 09616, MS 0899)
Review & Approval Desk for DOE/OSTI (Dept. 9612, MS 0612)